Pergamon

Bioorganic & Medicinal Chemistry, Vol. 3, No. 6, pp. 795–809, 1995

0968-0896/95 $9.50 + .00

0968-0896(95)00063-1

NMR Studies of the Post-Activated Neocarzinostatin Chromophore–DNA Complex. Conformational Changes Induced in Drug and DNA

Xiaolian Gao,[a]* Adonis Stassinopoulos,[b] Juan Gu[c] and Irving H. Goldberg[b]

[a]*Department of Chemistry, University of Houston, Houston, TX 77204-5641, U.S.A.*

[b]*Department of Biological Chemistry and Molecular Pharmacology, Harvard Medical School, Boston, MA 02115, U.S.A.*

[c]*Center for Biotechnology, Baylor College of Medicine, Houston, TX 77030, U.S.A.*

Abstract—The glutathione post-activated neocarzinostatin chromophore (NCSi-glu)–DNA complex was studied in detail by 2-D NMR spectroscopy. The complex is a model for understanding the sequence specific cleavage of DNA by the native neocarzinostatin chromophore (NCS chrom), a highly potent enediyne antitumor agent. NMR spectral analysis is presented for the free NCSi-glu, the free DNA duplex and the NCSi-glu–DNA complex. In addition to the previously reported structural details of the complex (Gao, X.; Stassinopoulos, A.; Rice, J. S.; Goldberg, I. H. *Biochemistry* **1995**, *34*, 40), we demonstrate that the binding of NCSi-glu in minor groove results in a patch of negatively charged surface covering the otherwise relatively neutral minor groove. The formation of the complex is largely driven by hydrophobic forces and the solvation of the polar surface of the complex. Comparison of the conformations of NCSi-glu and DNA duplex in their free and bound form reveals an induced mutual fit of DNA and NCSi-glu upon complex formation. The reduced NCS chrom represents a DNA binding motif for sequence specific recognition of DNA via intercalation and minor groove interactions.

Introduction

Neocarzinostatin chromophore[1] (NCS chrom) is the first member in a family of highly potent enediyne antitumor antibiotics that bind to specific DNA sequences and cause single and/or double strand lesions.[2] Among the enediyne compounds, NCS chrom and chromophores of kedarcidin,[2a] C-1027[2b] and maduropeptin[2c] are components of protein complexes, while calicheamicins,[2d] esperamicins[2e] and dynemicin[2f] are low molecular weight molecules directly isolated from eubacterial actinomycetes. Like other members in this family of antitumor agents, NCS chrom contains an enediyne core (Scheme 1), attached to which are several substituent groups: the cyclocarbonate moiety on C-4, the 2'-*N*-methyl-D-fucosamine (NMF) sugar on C-10 and the naphthoate (NPH) ring on C-11 (Scheme 1).[3] Nucleophilic addition by thiol reagents, such as glutathione, to the enediyne core of NCS chrom results in aromatization of the ring system and formation of the 2,6-biradical species.[3b,4] When bound to DNA, this highly reactive species abstracts hydrogens from deoxyribose sugar rings, resulting in formation of a tetrahydroindacene ring (THI, Scheme 1). Thus, oxidative single-stranded (ss) and to a lesser degree, double-stranded (ds) chain cleavage of DNA are induced by the drug.[1c,5] Ss cleavage has been most frequently observed at 5'- or 4'-positions of thymine residues. Specific cleavage sites have been identified in the event of ds cleavage. For instance, in the trinucleotide AG<u>X</u>·YC<u>T</u> (X = C or T and Y = G or A)

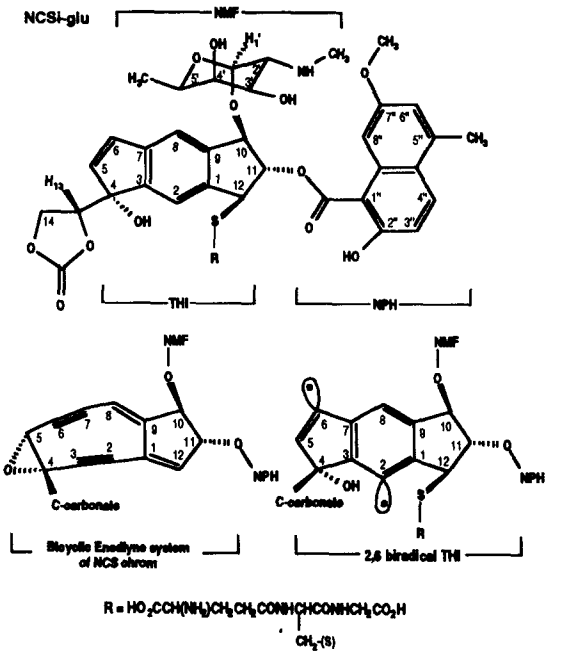

Scheme 1.

sites NCS chrom induces sugar damage at the 5'- or the 4'-position of the <u>T</u> residue and at the 1'-position of the <u>X</u> residue. A new mechanism of NCS chrom activation in the absence of thiol agents is proposed recently to account for the observation of the site-specific cleavage at a bulge site.[6] Other enediyne antibiotics have been shown to interact with DNA, causing ss and/or ds lesion

sites in target sequences.[5,7] Although the chemistry of the cleavage reactions is similar, the sequence specificity for various enediyne antitumor agents is distinctively different. There has been intensive effort in understanding the sequence selectivity of DNA cleavage by NCS chrom and other enediyne antitumor agents. This has led to the recent structural models for the post-activated NCS chrom–,[8] calicheamicin γI–[9] and esperamicin A_1[10]–DNA complexes derived from modeling or NMR/molecular dynamics simulations. Evidence has been obtained for NCS chrom, which shows that the binding occurs in the minor groove[11] with the NPH aromatic ring intercalating into the base stacks of DNA.[12] The binding of the enediyne core in the minor groove has been further examined by modeling studies in order to rationalize the observed sequence specific hydrogen abstraction.[8] It becomes clear that structural information at the atomic level is essential for the advancement of our understanding of NCS chrom–DNA specific interactions.

In this report, we describe a detailed NMR analysis of the glutathione post-activated NCS chrom (NCSi-glu)–DNA complex. The results of this study have been used to elucidate the structure of the complex using distance geometry and molecular dynamics simulation methods. A complete description of the structural features of the complex has been reported.[13] The heptamer DNA duplex (Scheme 2) used in this study contains an AGC trinucleotide site, which when embedded in a long DNA sequence, undergoes specific cleavage in the presence of NCS chrom and glutathione.[14] The activated NCS chrom abstracts one 5' hydrogen from T12 and the 1' hydrogen from C5, resulting in chain cleavage at the C11–T12 step and an abasic site at C5, which eventually leads to backbone lesion formation.[1c,5] The use of native NCS chrom in NMR studies of the complexes involving oligonucleotides is unsuitable, however, due to its high lability in aqueous solution. Our fluorescence binding studies indicate that NCSi-glu, which most closely resembles the biradical species of the drug (Scheme 1), serves as an analog of the native form.[13,14] Here we present an NMR analysis of conformational changes induced in NCSi-glu and DNA upon complex formation and the principles which are important for drug–DNA recognition and stabilization of the complex.

5'-	G1	G2	A3	G4	C5	G6	C7	
	•	•	•	•	•	•	•	
	C14	C13	T12	C11	G10	C9	G8	-5'

Scheme 2.

Results

NMR spectral analysis of the free NCSi-glu

Chemical shift assignments. Two-dimensional (2-D) TOCSY[15] and NOESY[15] spectra of the free NCSi-glu are shown in Figure 1. A combined analysis of the DQF-COSY,[15] TOCSY and NOESY spectra provides resonance assignments for all nonexchangeable protons of the free NCSi-glu (Table 1). These assignments are in general agreement with those obtained from a sample of NCSi-glu dissolved in 2 mM DCl/D_2O.[16] Spin connectivities of the NMF and THI moieties are traced from the TOCSY spectrum where typical patterns of cross peaks provide multiple bond coupling networks (Fig. 1A). For instance, NMF H-1' at 5.64 ppm (Fig. 1A) shows coupling cross peaks to H-2', H-3' and H-4',

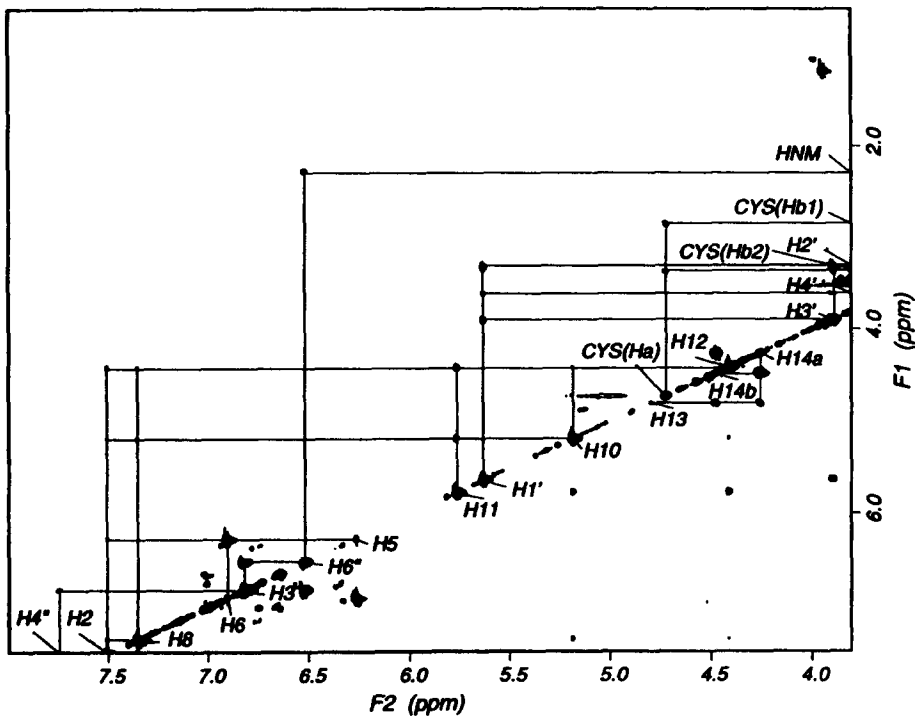

Figure 1. Expanded clean-TOCSY spectrum of the free NCSi-glu. Experimental conditions are given in the Experimental. Multiple-bond spin connectivities are indicated by solid lines while the corresponding assignments are give along the diagonal.

while THI H-2 at 7.51 ppm exhibits multiple coupling to nearly every proton which are in the plane of the THI ring system (H-8, H-5, H-10 and H-12). The assignment of the cyclocarbonate (H-13, H-14a and H-14b) and the peptide side chain protons (Ha and methylene Hb protons) are based on cross-peak patterns typical for the CH-CH_2 spin systems in the DQF-COSY spectrum. Several large coupling constants (> 7 Hz) are detectable from the DQF-COSY spectrum (data not shown). The large coupling between NMF H-2' and H-3' and the weaker couplings between H-1' and H-2' and between H-3' and H-4' are consistent with the axial orientation of the glycosidic linkage of the α-D-NMF moiety. The strong DQF-COSY cross-peaks correlating the cyclocarbonate H-13 with H-14a and Cys Ha with Hb-1 are accompanied by extremely weak cross peaks correlating H-13 with H-14b and Cys Ha with Hb-2. These measurements are related to the cyclocarbonate ring pucker and the orientation of the peptide side chain, indicating that the dihedral angles defined by H-13–C-13–C-14–H14b and Ha–Ca–Cb–Hb-1 are close to –30°.

NOE and conformation of the free NCSi-glu. A set of well-defined NOEs are observed in the NOESY spectrum (350 ms mixing time) of the free NCSi-glu.[17] These interproton contacts are qualitatively shown in Scheme 3 and listed in Table 1. NOEs correlating H-2 and H-11 of THI with Ha and Hb protons of the Cys residue and those correlating H-12 of THI with Ha protons of the Gly residue (Table 1) suggest that Cys residue is located close to the five membered ring while the Gly residue of the peptide side chain is close to the H-2 side of the THI ring. This orientation places the Glu residue pointing away from the THI ring. Indeed, there is no detectable NOE attributable to the resonances of the Glu residue. NOEs connecting the cyclocarbonate H-13 and H-14 methylene protons with THI H-2 and H-5, respectively, are present (Scheme 3, Table 1). These interresidue NOEs suggest that the hydrophobic edge of the cyclocarbonate moiety (H-13, H-14 protons) is facing inward towards the THI tricyclic ring, while the carbonate carbonyl group is pointing outward towards the solvent. The NMF sugar and the THI ring show a number of interproton interactions which are mostly related to the hydrophobic region (H-1', *N*-methyl, H-5' and 6'-methyl) and one side of the THI ring (H-11, H-10, H-8 and H-6) (Scheme 3). NMF H-1' and 2'-*N*-methyl show NOEs to H-11 and H-10, while H-5' and 6'-methyl exhibit NOEs to H-6 and H-8. This set of NOEs demonstrates the nearly parallel orientation of the NMF sugar and the long axis of the THI ring with the NMF 6'-methyl located in the vicinity of the H-6 of THI and H-2' and the two hydroxyl groups of NMF pointing towards the solvent (Scheme 3). Only one weak NOE is related to the NPH aromatic ring, i.e. the one between H-3" of NPH and Ha protons of Gly. Thus, the NPH ring appears to adopt either a random conformation or a conformation that does not make contact with other moieties of NCSi-glu. Thus far the assigned NOEs have been interpreted within the context of intramolecular contacts, although the possibility that some of these NOEs may arise from intermolecular associates can not be excluded at this time. Nonetheless, it is indisputable that the free NCSi-glu exists in a stable conformation in a D_2O solution containing 27% methanol, 20 mM NaCl, 5 mM PO_4.

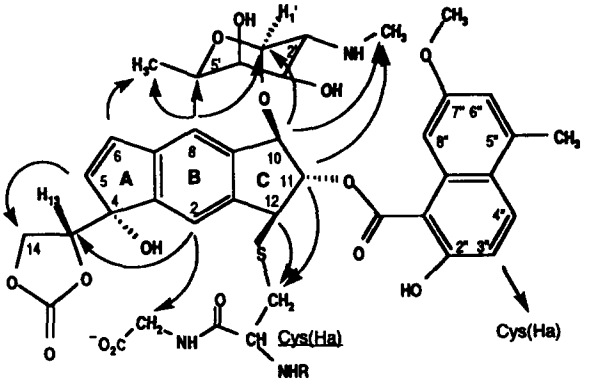

Intramolecular NOEs of the free NCSi-glu

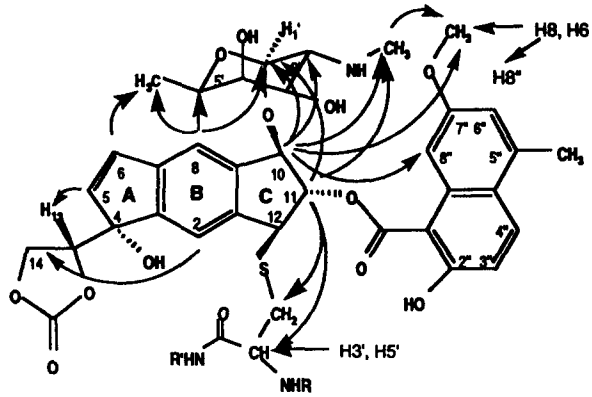

Intramolecular NOEs of the bound NCSi-glu

Scheme 3.

NMR spectral analysis of the free duplex

A complete data set containing spectral information about through bond and through space connectivities is recorded for the free duplex. Examples of the 2-D DQF-COSY, NOESY and the proton detected ^1H–^{31}P COSY[18] spectra for the free duplex (Scheme 2) are shown in Figures 2A–4A, respectively. The combined analysis of these spectra led to the assignment of the majority of ^1H and ^{31}P resonances (Table 2). The nonself-complementary heptamer duplex exhibits a typical spectral pattern similar to what is described for a B-type helix.[19] Five imino protons are observed in aqueous solution in the 12.7–13.1 ppm (four resonances) and 13.89 ppm regions. Each of the four resonances around 13 ppm show NOE connectivities to a pair of C amino protons (data not shown). This is indicative of Watson–Crick C·G base pair formation. NOE connectivities between intra- and interresidue proton resonances of DNA base and sugar moieties are well-defined. The spectral region showing H-2' and H-2" (F1) and base proton (F2) NOEs is plotted in Figure 2A, which demonstrates the interactions of base to H-2' and H-2" protons of the same and the preceding residues. The

Table 1. [1]H Chemical shifts of the free NCSi-glu and the chemical shift difference of NCSi-glu in the free and bound form[a]

NPH	H3"	H4"	HNM	H6"	H7"M	H8"			
ppm	6.82	7.75	2.28	6.53	3.58	8.31			
Δppm	*1.17*	*0.47*	*0.27*	*0.99*	*0.98*	*1.61*			
NME	H1'	H2'	H2M	H3'	H4'	H5'	HFM		
ppm	5.64	3.33	2.83	3.90	3.63	3.69	0.99		
Δppm	*-0.67*	*0.14*	*-0.04*	*0.14*	*0.18*	*0.54*	*0.03*		
THI	H2	H5	H6	H8	H10	H11	H12	H13	H14a, H14b[b]
ppm	7.51	6.27	6.91	7.36	5.19	5.77	4.41	4.80	4.27, 4.47
Δppm	*0.00*	*-0.12*	*-0.02*	*-0.29*	*-0.25*	*0.20*	*-0.44*	*-0.27*	*-0.23, -0.03*
CYS	HA	HB1,HB2[b]							
ppm	4.72	2.86, 3.37							
Δppm	*0.14*	*0.26, 0.33*							

[a]Chemical shift assignments of the free NCSi-glu were obtained from the NOSEY spectrum.
Chemical shift assignments of NCSi-glu in bound form were obtained from the 150 ms NOSEY of sample II recorded at 5 °C.
Δ(ppm) = ppm(free NCSi-glu) – ppm(bound NCSi-glu). A positive value indicates an upfield shift upon complex formation.
For the free NCSi-glu Gly(Ha) 3.02; Glu(Ha) 3.61; Glu(Hb1, Hb2) 2.05, 2.43; Glu(Hg1, Hg2) 2.06, 2.07.
[b]Non-stereospecific assignments.

relative intensity of these NOEs are, in general, consistent with an unperturbed B-type right handed helix. The DQF-COSY and COSY-35 (data not shown) cross-peaks, such as those shown in Figure 3A, reveal that $J_{H1'-H2'}$ couplings are slightly larger than $J_{H1'-H2''}$ couplings while those of $J_{H3'-H2''}$ and $J_{H3'-H4'}$ are weak or absent. This spectral pattern is consistent with that of a C-2'-endo type sugar pucker.[20] A total of 12 ^{31}P resonances in the free duplex are assigned from the bond correlation of H-3'-P, H-4'-P and H-5',5"-P (Fig. 4A and Table 2). The chemical shifts of the ^{31}P resonances, which fall into a narrow region of 0.6 ppm, are consistent with what is expected for a canonical B-helix.[21]

NMR spectral analysis of the NCSi-glu–DNA complex

Formation of the NCSi-glu–DNA complex was determined by the disappearance of the sharp resonance lines of the free drug when free DNA duplex was added to a sample of NCSi-glu. A mixture sample containing the free DNA duplex and NCSi-glu–DNA complex in 1:1 ratio (sample I) and a sample containing only the complex (sample II, one NCSi-glu per duplex) were prepared.[13] Exchange cross-peaks in the NOESY spectra of the mixture sample I correlate proton resonances in the free and the bound form and is useful for proton assignments or confirming proton assignments of the complex. The shifted resonances in the complex, such as H-1' protons of G2, G4, C11, T12 and C13, are, therefore, unambiguously assigned from the corresponding exchange cross-peaks in the NOESY spectrum (250 ms mixing time) of sample I. The relative intensities of these exchange cross peaks with regard to the diagonal peaks range from 20–50%, which places a rate limit of 0.8–2 s^{-1} to the exchange process.[22] Chemical shift assignments of the ^{1}H and ^{31}P resonances in the complex have been completed and are reported elsewhere.[13] A comparison of the chemical shifts of the ^{1}H resonances in the complex with those in the free duplex is given in Table 2. Large changes in the proton chemical shifts upon complex formation involve mainly resonances of G2, G4, C11 and T12 residues (Table 2).

Base pair formation. Five imino proton resonances observed in the spectra recorded in 90% H_2O/D_2O solution have been assigned to G2, G4, G6, G10 and T12 residues. The imino protons of the central binding site (A3·T12, G4·C5 and C5·G10) exhibit NOEs to A H-2 or C amino protons, indicating that base pair formation at these positions is not perturbed upon complex formation. The imino proton resonances of G2·C13 (12.60 ppm) and G6·C9 (13.07 ppm) are relatively broad and their NOEs to amino protons are not as strong as those seen in the free duplex. However, the chemical shifts of these imino protons and the observation of hydrogen bonded amino proton resonances at 8.41 and 8.09 ppm and non-hydrogen bonded amino proton resonances at 6.97 and 6.33 ppm of C13 and C9 residues suggest that these bases are also paired in the complex. The line broadening of the G2 and G6 imino proton resonances may be due to local motion induced by binding or simply because the binding causes the penultimate base pair to be more prone to terminal fraying effect.

Sequential connectivities. ^{1}H resonances in the complex are assigned by analyzing intra- and inter-

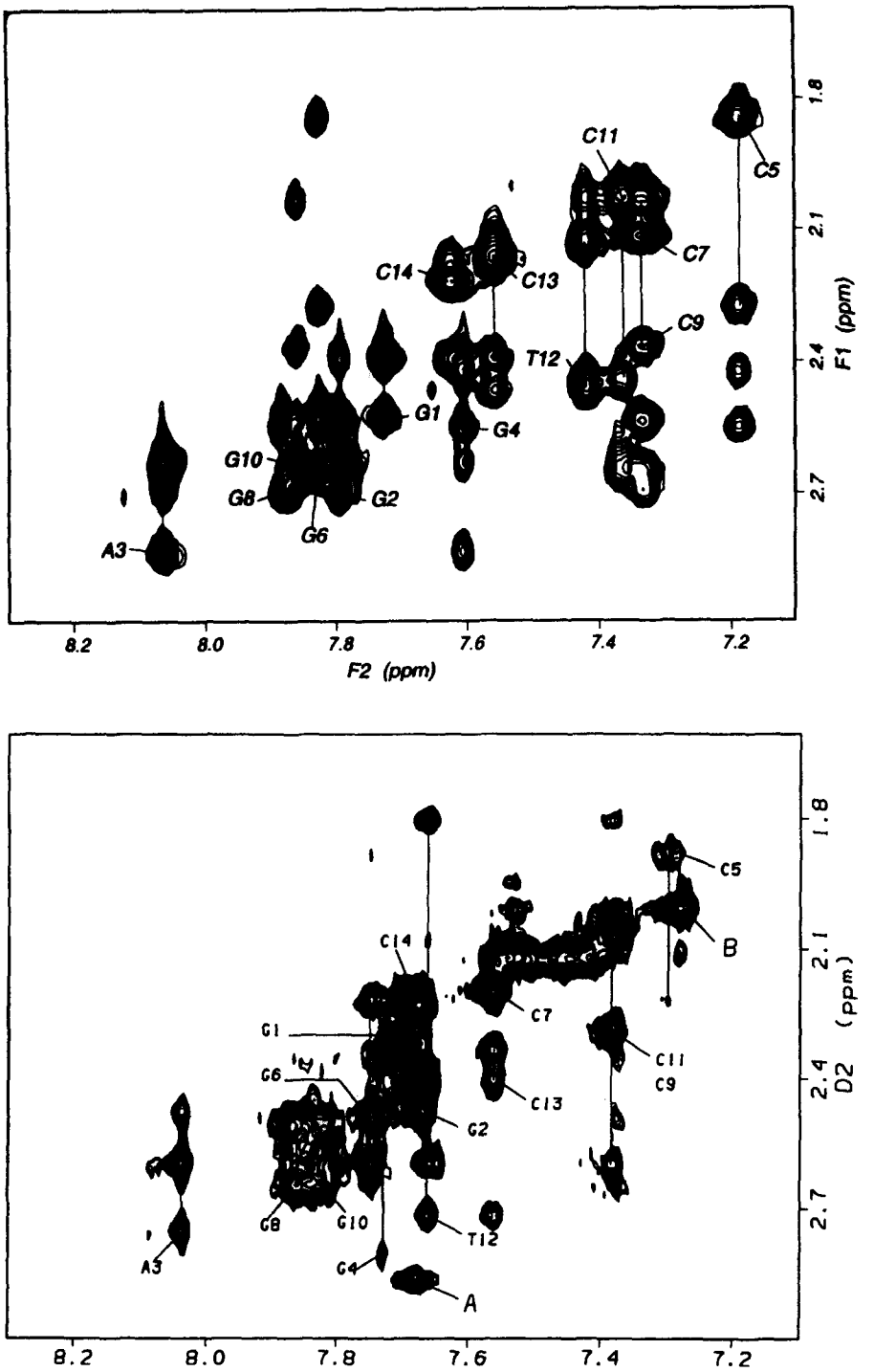

Figure 2. Expanded NOESY spectra covering base proton resonances (F2) and sugar H-2' and H-2" proton resonances (F1). Detailed experimental conditions are given in the Experimental. (A) Spectrum of the free duplex with a mixing time of 250 ms. The intraresidue base to sugar proton NOEs are marked by solid lines and the residue number. (B) Spectrum of the NCSi-glu–DNA complex with a mixing time of 150 ms. In addition to the indicated intraresidue NOEs, peak A is the NOE from A3 H-2 to NCSi-glu H-2M and peak B is the NOE from NCSi-glu H-4" to NCSi-glu H-NM.

residue NOEs in combination with through bond connectivities. An expanded NOESY spectrum containing NOE cross peaks of base proton resonances (F2 dimension) and H-2' and H-2" sugar proton resonances (F1 dimension) is drawn in Figure 2B. Intensities of intraresidue base-sugar H-1' NOEs are weak, excluding the presence of a *syn*-glycosidic configuration in the complex. The sequential NOEs of the non-terminal residues in Figure 2B and in the base-H-1' spectral regions are generally weak while those linking A3–G4, C5–C6 and C9–G10 steps are too weak to be observed. This is in contrast to what is observed in the free duplex, where sequential NOEs exhibit weak to moderate intensities (base-H-1') and moderate to strong intensities (base-H-2',H-2"). The reduction in sequential NOE intensities in the complex is suggestive of

prolonged separation between adjacent base pairs, which may be attributed to intercalation of ligand molecules and/or unwinding of the DNA duplex.

^1H–^1H and ^1H–^{31}P couplings. A 2-D DQF-COSY spectrum displaying H-1'–H-2' couplings of the complex is shown in Figure 3B. Except for the overlapped H-2' and H-2" resonances of G2, C7, C13 and C14 residues, the H-1'-H-2' coupling cross peaks are observed for Gl, A3, G4, G6, G8, G10, C11 and T12 residues but not for C5 and C9 residues. The chemical shifts of C11 H-2' and H-2" protons are inverted (H-2" at 2.07 ppm is shifted to upfield compared to H-2' at 2.29 ppm). Comparatively, H-1'–H-2" coupling cross-peaks are either weak or absent. These results, in conjunction with the absent couplings of H-3'–H-4' and H-3'–H-2",

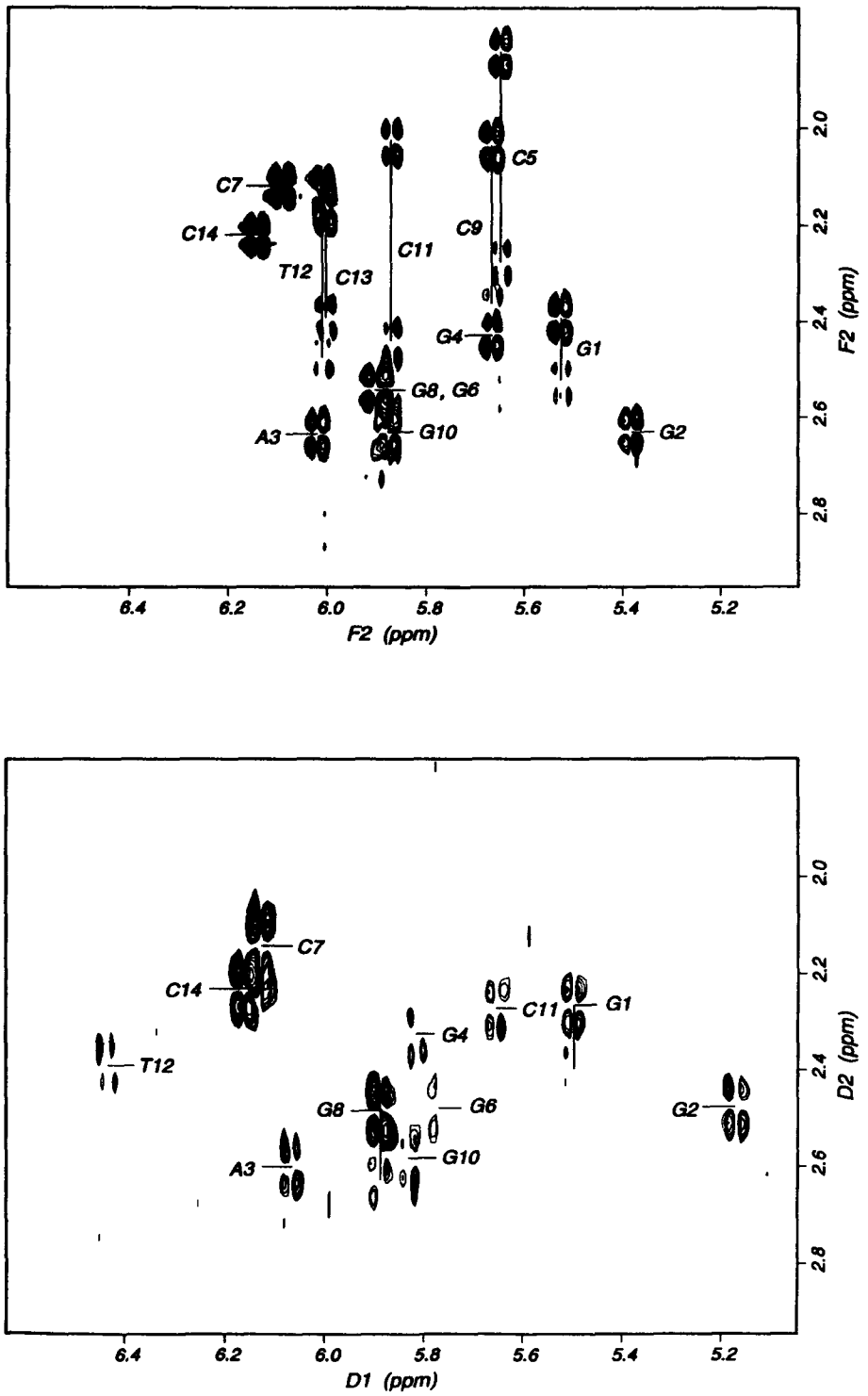

Figure 3. Expanded DQF-COSY spectra illustrating scalar couplings of H-1' (F2) to H-2' and H-2" (F1) protons as indicated by solid lines and residue numbers. Experimental conditions are given in the Experimental. (A) Spectrum of the free duplex. (B) Spectrum of the NCSi-glu–DNA complex. Note that in each spectrum, the coupling cross peaks of H-1'–H-2" are either absent or much weaker than those of H-1'–H-2'.

indicate that most sugar residues are in conformations close to the C2'-endo configuration.[20] The missing coupling cross-peaks for the C5 and C9 residues and the weak signals in the TOCSY spectra (data not shown) may result from line broadening in the complex.

The ^{1}H detected ^{1}H–^{31}P COSY of the NCSi-glu–DNA complex is shown in Figure 4B. The two ^{31}P resonances shifted mostly downfield are assigned to the phosphate linking A3–G4 and C11–T12. The chemical shift differences of ^{31}P resonances between the complex and the free duplex are given in Table 2. Since ^{31}P chemical shifts are sensitive to bond and torsion angles connecting P to coordination atoms,[21] the significant shifts of ^{31}P resonances upon complex formation are strong evidence that the backbone conformation of the complex is drastically different from that of the free duplex. The perturbation in ^{31}P chemical shifts is in

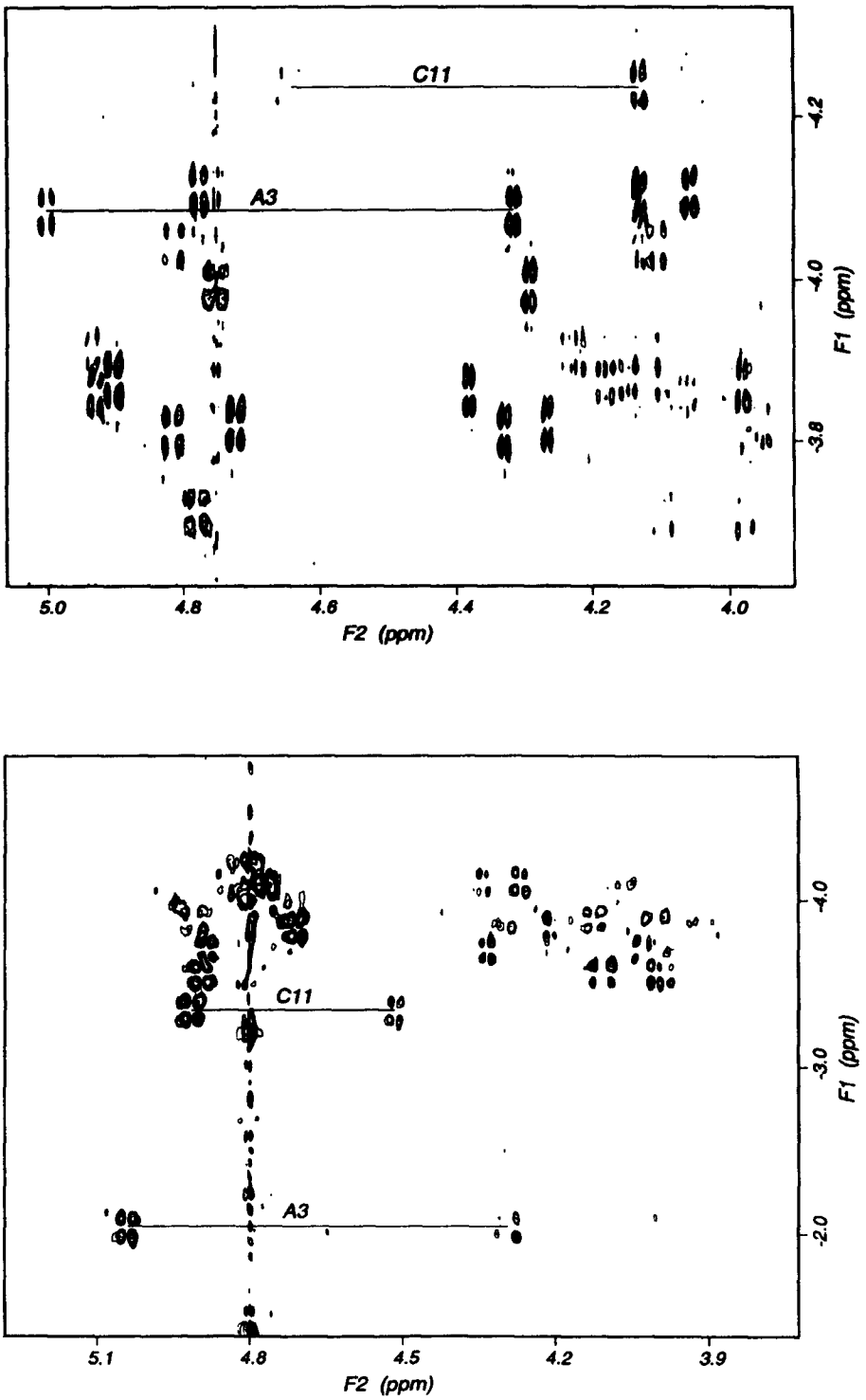

Figure 4. Proton detected ^{1}H–^{31}P COSY spectra illustrating scalar couplings of H-3', H-4' and H-5',H-5" (F2) with backbone phosphorous resonances (F1). The assignments of proton and ^{31}P resonances are given in Table 1 and Ref. 13. The ^{1}H–^{31}P correlations of A3 H-3' to $^{31}P_{A3\text{-}G4}$ and C11 H-3' to $^{31}P_{C11\text{-}T12}$ are indicated, demonstrating the large perturbation in ^{31}P chemical shifts upon complex formation.

Table 2. Proton assignments of the free DNA duplex and the chemical shift difference of DNA duplex in the free and bound form

	Imino		Amino(b)		Amino (nb)		H8/H6		H2/H5		H1'		H2'		H2"		H3'		H4'		P31	
	DNA	d(ppm)	DNA	d(ppm)	DNA	d(ppm)	DNA	d(ppm)	DNA	d(ppm)	DNA	d(ppm)	DNA	d(ppm)	DNA	d(ppm)	DNA	d(ppm)	DNA	d(ppm)	DNA	d(ppm)
G1							7.73	0.03			5.52	0.04	2.39	0.08	2.53	0.10	4.72	0.03	4.09	0.05	-3.82	0.00
G2	12.86	0.26					7.79	0.12			5.37	0.21	2.63	0.15	2.70	0.22	4.93	0.07	4.25	0.05	3.86	-0.17
A3							8.06	0.02	7.69	0.01	6.01	-0.04	2.63	0.03	2.84	0.09	5.00	-0.02	4.38	0.05	-4.09	-2.05
G4	12.79	1.48					7.61	-0.11			5.66	-0.17	2.42	0.08	2.55	-0.26	4.89	0.22	4.30	-0.12	-3.87	
C5			8.18	0.00	6.33	-0.37	7.19	-0.11	5.18	-0.12	5.64	0.10	1.84	-0.03	2.28	0.06	4.75	0.02	4.10	0.05	-3.99	
G6	12.96	-0.11					7.83	0.08			5.88	0.11	2.54	0.05	2.65	0.05	4.89	0.00			-3.87	-0.30
C7							7.33	-0.23	5.29	-0.34	6.08	-0.03	2.12	-0.01	2.12	-0.01	4.43	-0.01	3.95	-0.05		
G8							7.88	0.02			5.90	0.01	2.54	0.03	2.70	0.04	4.76	0.01	4.18	0.03	-4.11	
C9			8.40	0.01	6.52	0.19	7.33	-0.06	5.29	-0.02	5.66	0.03	2.03	-0.17	2.37	0.01	4.81	0.06			-3.81	
G10	13.05	0.26					7.86	0.05			5.87	0.05	2.64	0.05	2.64	0.00					-3.91	
C11			8.12	0.37	6.55	0.00	7.36	-0.02	5.28	-0.03	5.86	0.22	2.03	-0.26	2.44	0.37	4.64	-0.16	4.16	0.04	-4.24	-0.91
T12	13.89	0.71					7.42	-0.24	1.55	-0.26	6.00	-0.44	2.13	-0.28	2.46	-0.26	4.81	-0.18	4.12	-0.41	-4.04	-0.48
C13			8.48	0.07	7.01	0.04	7.56	0.00	5.69	0.06	6.00	-0.11	2.16	-0.04	2.39	0.05	4.77	-0.11	4.10	-0.17	-3.71	
C14							7.82	-0.06	5.71	-0.10	6.13	-0.01	2.22	-0.01	2.22	-0.01	4.48	-0.02	3.96	-0.29		

[a]Proton assignments of the free DNA duplex in D_2O were obtained at 10 °C, sample solution contained 5 mM PO_4, pH was 5.8.
Exchangeable proton assignments were obtained from a mixture of 1:1 complex:free duplex at 5 °C, sample contained 5 mM PO_4, 20 mM NaCl. pH was 5.5.
Δ(ppm) = ppm(free DNA) – ppm(complex),[13] a positive value indicates that the chemical shift of the free DNA duplex resonance is down field shifted relative to that of this resonance in the NCSi-glu–DNA complex.

accordance with the observed weakening in sequential NOEs of the complex (*vide supra*).

NCSi-glu proton assignments in the complex. Only one set of proton resonances corresponding to NCSi-glu is observed in the complex. The assignments rely on the identification of spin–spin couplings and NOE analysis. NCSi-glu in the bound form exhibits spin connectivities similar to those of the free form. For instance, THI H-6 is scalar coupled to H-5 and shows an NOE to H-8; NMF sugar H-1' is scalar coupled to H-2' (TOCSY) and shows a strong NOE to H-10. Large couplings are observed between Ha and Hb-1 of the Cys residue and between H-2' and H-3' of the NMF residue. Thus, the chair form of the NMF sugar remains unchanged upon complex formation. All proton resonances of the bound NCSi-glu (except for Gly and Glu residues and the exchangeable amide/amine protons) are assigned in a way similar to what is described in the spin assignments of the free NCSi-glu.[13]

Chemical shift comparison with the free NCSi-glu. Comparison of the ^1H chemical shifts of the bound NCSi-glu with those of the free form is given in Table 1. The resonances of the naphthoate ring exhibit the most significant upfield shift (0.27–1.61 ppm) upon complex formation. These upfield shifted resonances in the bound NCSi-glu are an indication of intercalation by the naphthoate ring. On the other hand, the trend and origin of the various ^1H chemical shifts in other portions of NCSi-glu are less clear. These variations could be due to a number of factors, such as change in conformation of the drug itself and/or in the surrounding environment upon complex formation.

NCSi-glu intramolecular NOE assignments. NCSi-glu in the complex manifests 20 intramolecular NOEs which correlate various moieties (Scheme 3, Table 1). THI H-

11 shows NOEs to Cys Hb-1 and Hb-2 at equally weak intensities, providing the orientation of the peptide side chain in relation to the THI ring. THI H-2 and H-5 are in contact with H-14* (degenerate H-14 methylene protons) and H-13 in the complex, respectively. This is a reversed NOE pattern compared to what is observed in the free NCSi-glu. To establish these proton contacts the cyclocarbonate ring has to undergo a counter clockwise rotation by larger than 90° along the C4–C13 bond to position the carbonate carbonyl partially inward towards the THI ring. This orientation, unique to the complex, results in the formation of a hydrophobic binding surface where H-13 and H-14 protons align with THI H-2 and H-12 protons. The NOEs between the THI and the NMF sugar moieties in the complex are most similar to those of the free NCSi-glu (*vide supra*). The difference is that THI H-10 and H-11 in the complex show weak NOEs to H-2' of the NMF sugar, while these NOEs are absent in the free NCSi-glu. Therefore, the relative orientation of the NMF sugar and the THI ring is only slightly adjusted in the complex. There are a number of interresidue NOEs involving proton resonances of NPH (Scheme 3), such as those correlating THI H-6, H-8 and H-10 with H-7M (methoxy protons) of NPH. A weak NOE is detected between NMF sugar H-1' and NPH H-7M. These additional NOEs in the complex suggest that the NPH ring has undergone a major conformational transition to facilitate complex formation.

Intermolecular NOE assignments. Intermolecular interproton contacts are the most important spectral features for the structure elucidation of the NCSi-glu–DNA complex. Many of these NOEs are identified during spectral assignment, while some of them are assigned by a semiautomated cross peak assignment procedure.[13] These intermolecular NOEs involve THI, NMF and NPH residues of NCSi-glu and A3, G4, C11, T12, C13 of the DNA duplex. The NPH protons exhibit several NOEs to DNA base protons, such as A3 H-8, C11 H-5 and H-6 and T12 H-5 methyl and H-6, demonstrating a clear pattern of NPH intercalation between A3·T12 and G4·C11 base pairs. The alignment of the NPH ring at the intercalation site is defined by several NOEs, such as those of H-7M to C11 H-1' (m), H-2' and H-2" (w) and those shown in Figure 5, where H-2-0H of NPH exhibits NOEs to A3 H-2' and H-2" (H-2-OH to A3 H-1' NOE also exists, data not shown). These interproton interactions indicate that the long axis of NPH is proximately parallel to that of the adjacent base pairs with the methoxy group pointing towards the T12 strand. The contacts between the NMF sugar and the DNA duplex are reflected in NOEs connecting NMF H-1', H2M (*N*-methyl) and HFM (5'-methyl) with H-1' and backbone H-4', H-5', 5" protons of T12 and C13 residues. Additionally, a strong NOE cross peak is assigned to NMF H-2M and A3 H-2. In a right handed duplex, H-1', H-4' and adenine H-2 protons are located in the minor groove. Therefore, NOEs related to NMF reveal that the sugar moiety binds in the minor groove at a site adjacent to A3, T12 and C13. The interactions between the THI ring and the duplex are found at two locations. The H-6 and H-8 protons from one side of the unsaturated ring of THI (Scheme 1) show several NOEs to H-4', H-5' and H-5" protons of T12 (moderate to weak), while H-10, H-11 and H-12 from one side of the saturated ring of THI show NOEs to A3 H-2, T12 H-1' and G4 H-1' (moderate to weak). This set of NOEs permits the placement of the THI ring in the minor groove with ring A-C aligning in a 3'-5' (T12–C11) fashion. H-6 and H-2 of NCSi-glu are the sites of free radical formation in the hydrogen-abstraction 2,6-biradical species (Scheme 1). In the complex, H-6 is found to give NOEs to H-4', H-5' and H-5" of T12 with moderate to weak intensities, while H-2 does not show any detectable NOEs to non-exchangeable DNA protons.

Discussion

In this article, we present an NMR spectral analysis of the free NCSi-glu, the free DNA duplex and the NCSi-glu–DNA complex. These results and their comparisons provide qualitative representations of the stable conformations for each of the above three molecular entities. Using combined distance geometry and molecular dynamics simulations we have established

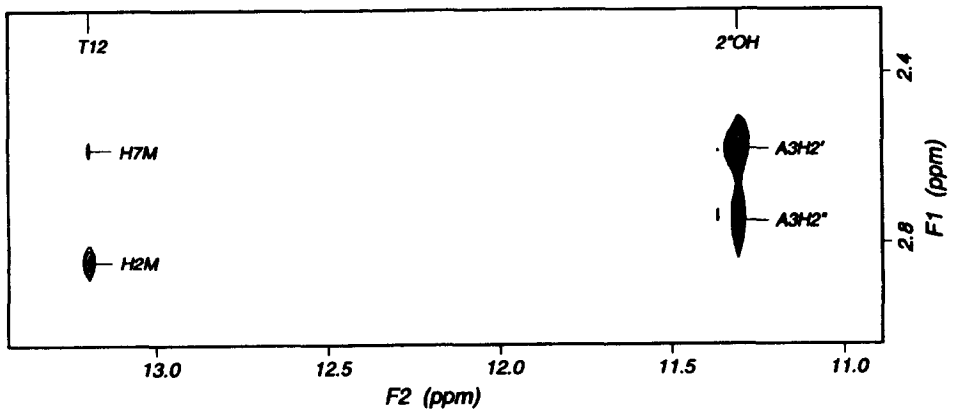

Figure 5. Expanded NOESY spectrum (200 ms mixing time) of the NCSi-glu–DNA complex recorded in 90% H_2O/10% D_2O. The NOE cross-peaks are assigned to contacts between the T12 imino proton resonance and the NCSi-glu methyl proton resonances (NMF H-2M and NPH H-7M) and between the NCSi-glu naphthoate hydroxyl (2"-OH) and the DNA sugar proton resonances (A3 H-2' and H-2").

the three dimensional structure of the NCSi-glu–DNA complex.[13] Structural drawings of the complex showing views into the minor groove and from the side of the minor groove are given in Figure 6. The discussion below emphasizes the comparison of the free NCSi-glu and DNA with those in the bound form, respectively, and the structural features of the NCSi-glu–DNA complex as revealed by this NMR study.

NMR results and structure features of the NCSi-glu–DNA complex

NMR spectral analysis reveals (a) chemical shift perturbation of ^{1}H and ^{31}P resonances at C11–C13 and A3–C5 sites upon complex formation; (b) proton–proton contacts between DNA bases (A3·T12 and G4·C11) and the NPH moiety; (c) many other interproton interactions between DNA and NCSi-glu. These results permit positioning of NCSi-glu in the minor groove adjacent to the A3G4C5·C11T12C13 site with the NPH ring intercalating into the A3G4·C11T12 step (Fig. 6). This mode of binding is consistent with what is proposed for the native NCS chrom interaction with DNA[11,12] and the results of modeling studies of NCSi-glu–DNA complexes.[8a,c] The NOEs correlating H-6 of THI with the H-4' and H-5' of the T12 residue, and NOEs involving protons of the THI ring and protons in the minor groove of DNA unequivocally define the orientation of the THI moiety and place the H-2 of NCSi-glu close to the H-1' of C5 (Fig. 6). These results are in agreement with deuterium abstraction experiments.[2,3] The stacking of the C11 sugar on the THI ring may be the origin of the upfield shifted H-2" resonance. Examination of intermolecular NOEs in the complex reveals the important contribution from van der Waals hydrophobic interactions between NCSi-glu and DNA. The color coded electrostatic surface drawings in Figure 7 show that the binding interfaces at the intercalation and minor groove sites are neutral (white and light blue). In contrast, the solvent exposed surface of NCSi-glu is negatively charged (reddish, Fig. 7). Thus, the binding of NCSi-glu to DNA results in a negatively charged patch covering the otherwise relatively neutral minor groove, indicating that the complex formation is largely driven by hydrophobic forces and the solvation of the polar surface of the complex.

Conformational transition of NCSi-glu from free to bound form

The presence of a set of well defined NOE correlations in the free NCSi-glu suggests that the molecule adopts a stable conformation in an aqueous solution, although the orientation of the NPH moiety is inconclusive. The schematic drawings of these NOEs (Scheme 3) demonstrate the relative orientation of the NMF sugar, the cyclocarbonate and the peptide side chain with regard to the THI ring. When the complex is formed, the conformational change in NMF and THI appears to be trivial as shown by a similar set of NOEs in either the free or the bound form (Scheme 3). However, the cyclocarbonate ring, the peptide side chain and the NPH aromatic moiety adopt a significantly different conformation in the complex. The cyclocarbonate ring of the free NCSi-glu has the hydrophobic edge (H-13, H-14a and H-14b) facing the THI ring and the polar carbonate group projecting towards the outer surface. In contrast, the cyclocarbonate ring in the complex has the hydrophobic edge facing outwards. The reason for this conformational transition is simple when the structure of the complex is examined (Figs 6 and 7). The orientation of the cyclocarbonate ring relative to the THI ring extends the hydrophobic surface of NCSi-glu along the direction of the THI ring, thus, enhancing the recognition of NCSi-glu in the minor groove of DNA. The peptide side chain in the free NCSi-glu is in close proximity to H-12 (the Cys residue) and H-2 (the Gly residue). In the complex, only the Cys residue is well defined, and this residue does not make contacts with H-12 (Scheme 3). Although the peptide side chain is not included in the structure shown in Figure 6, NMR results indicate that this residue may be quite flexible and does not have a stable bound conformation. The structure of the NCSi-glu–DNA complex shows that the THI and NMF moieties are well-positioned in the minor groove, leaving little room in the minor groove to accommodate the peptide side chain. Thus, the observed local motion at the C5 and G6 residues is likely due to the flanking peptide residues. Most notably, complex formation results in significantly different alignment of the NPH ring, which is not well-defined in the free form, but is confined in a stable conformation in the complex. As shown in Figure 6 and Scheme 3, the bound form of NPH protrudes into the DNA bases with the methoxy group and H-8" in close proximity to the THI ring.

Conformational transition of the duplex from free to bound form

NMR analysis of the free DNA duplex indicates a typical spectral pattern that is characteristic of a B-family helix. In comparison, NMR spectra of the complex exhibit many irregular patterns. The most significant spectral features are the weak or absent sequential NOEs that connect the base to adjacent sugar H1' protons and the largely shifted imino proton and ^{31}P resonances around the AGC site. These are typical spectral patterns of an intercalation complex. The conformation of the complex is well defined by a large set of intermolecular NOEs. A canonical B-DNA duplex and the DNA duplex in the NCSi-glu–DNA complex drawn in boxed form are shown in Figure 8A. The vertical view into the minor groove illustrates the elongation of the helix, especially at the AG (red-yellow) and CT (magenta-blue) sites and base buckle and tilt at the intercalation site. The view looking down the helix in Figure 8A demonstrates the unwinding of the helix (the two ribbons could not complete the circle in the complex) and base displacement relative to the helical axis. The base position displacement is most

Figure 6. A representative structure of the NCSi-glu–d[GGAGCGC]·[GCGCTCC] complex derived from NMR restraints using distance geometry and molecular dynamics simulations.[13] The left drawing shows the front view of the minor groove of DNA, in which the NCSi-glu resides. The binding site is indicated. The right drawing is a site view of both grooves, illustrating the intercalation of the NPH ring in between the A3·T12 and G4·C11 base pairs.

Figure 7. A surface electrostatic charge display of the DNA duplex and the NCSi-glu as in the complex.[30] Red and blue represent negative and positive charge density, respectively [charge parameters are from the Quanta program (Molecular Simulations Inc.)]. DNA duplex is viewed from the minor groove, which is essentially neutral. The interfaces between NCSi-glu and DNA are indicated. NCSi-glu undergoes a conformational transition when bound to DNA. The bound NCSi-glu adopts a conformation which complements the neutrality of the minor groove of DNA on one side and presents a polar, negatively charged potential on the solvent exposed surface.

Figure 8. The comparison drawing of the DNA duplex in the complexed form (left) and the canonical B-DNA duplex (right) generated from the Quanta program. The block-ribbon representations are produced using the GRASP program.[29] The four DNA bases are color coded according to type: A is red, C is magenta, G is yellow and T is blue (A). The top drawings show the elongated duplex and the intercalation site in the complex. The bottom drawings show the unwinding of the duplex by noting that the ribbons are ends-open in the complexed DNA duplex. Base stacks are mostly B-type in the complex, although there is apparently some variation (B). A display of base stacking patterns at dinucleotide steps of G2•C13/A3•T12 (top), A3•T12/G4•C11 (middle) and G4•C11/C5•G10 (bottom). The comparison between the DNA in the complex and the B-DNA demonstrates the displacement of the DNA bases in order to accommodate the intercalator NCSi-glu. The movement of the A3•T12/G4•C11 (middle) in the complex is quite dramatic compared to that of the canonical B-DNA.

significant at the point of NPH ring insertion (Fig. 8B). At the adjacent sites of intercalation, the pattern ofbase stacking in the complex is rather similar to that in typical B-DNA (Fig. 8B). These results and structures of several other ligand-DNA complexes[23] are compelling evidence for the flexible helical duplex of DNA.

Concluding remarks

This NMR study of the NCSi-glu–DNA complex and the comparison of the free forms of NCSi-glu and DNA with the complex provides a basis for 3-D structure elucidation of the NCSi-glu–DNA complex.[13] The binding of NCSi-glu to DNA is accompanied by mutual adjustment of the conformations of the free DNA duplex as well as the free NCSi-glu. NMR results define the alignment of the THI ring, which correlates well with the sequence specificity of the ds cleavage at the AGC site and thus, permit the deduction of a similar orientation for the enediyne core in the minor groove of DNA. Furthermore, this NMR analysis reveals the critical role of various substituents and their interaction with DNA in modulation of the formation of DNA lesion sites. The many specific contacts between the non-THI ring protons of NCSi-glu and those of DNA further illustrate that the binding of the enediyne ring to DNA is guided by the attached substituent groups. Similar observations have been reported in other enediyne antitumor agent–DNA complexes, such as those involving the calicheamicins and esperamicins.[9,10b] A new aspect revealed by this study is the realization that the NPH, NMF sugar and the THI tricyclic ring, chemically bound as such, is a DNA binding motif that recognizes specific DNA sequences, such as the AGC site. A variety of synthetic analogs may be developed to derivatize this structural motif. For instance, C-14 of the cyclocarbonate and N-2 of the NMF sugar may be potential sites for chemical modification by functional groups, which can further extend in the minor groove of DNA and are capable of selectively binding and/or cleaving specific DNA sequences.

Experimental

Preparation of the NCSi-glu–DNA complex

NCSi-glu was synthesized and purified as reported.[16b] The two heptanucleotide strands were chemically synthesized and purified by reversed-phase HPLC as described previously.[24] The annealing of the two strands at room temp. was monitored by ^{1}H NMR. The resulting DNA duplex was dissolved in 5 mM PO_4 and 0.1 mM EDTA (all salts used for NMR samples are in sodium form unless otherwise indicated) and gradually added to a sample of NCSi-glu dissolved in d_4-MeOH at 15 °C. The disappearance of the sharp signals of the free NCSi-glu and the shifted DNA imino proton resonances (*vide infra*) are markers for complex formation. Two samples were generated for NMR studies. Sample I contains 50% 1: 1 NCSi-glu–DNA complex and 50% free duplex, while sample II contains > 92% 1:1 NCSi-glu–DNA complex (percentage estimated from 1-D NMR data). These samples have a concentration of ~0.3 mM in 5 mM PO_4 and 0.1 mM EDTA, pH 5.5–5.8 (spectra were invariant in the pH range of 5.5–7.0). pH was adjusted using either an HCl or an NaOH solution and was uncorrected for readings in D_2O.

NMR experiments

NMR experiments were performed on spectrometers of 600 MHz at the U. of Houston and 750 MHz at Bruker Analytische Messtechnik GMBH (Bruker, Germany). For the DNA duplex and the NCSi-glu–DNA complex, D_2O (99.96%, Cambridge Isotopes Inc.) or 10% D_2O/90% H_2O were used as solvents for observation of non-exchangeable and exchangeable protons, respectively. Proton chemical shifts were referenced to the HOD resonance (4.70 ppm at 25 °C, temperature correction factor –0.0109 ppm °C^{-1}). ^{31}P chemical shifts were referenced relative to an external trimethyl phosphate in an aqueous solution containing 0.1 M NaCl (pH 6.5). All 2D NMR data were obtained with simultaneous detection in F2 and TPPI[25] phase cycling in F1 dimension, respectively. The States–Ruben–Haberkorn[26] phase program was used for the COSY-35 and ^{1}H–^{31}P correlation spectra. NMR data were processed using the FELIX 2.3 program (Biosym Technologies, Inc.) on an INDIGO/ELAN workstation (Silicon Graphics Computer Systems) and the UXNMR program (Bruker Instruments Inc.).

(a) NMR spectra of the free NCSi-glu. NMR spectra of the free NCSi-glu dissolved in 0.15 mL d_4-MeOH and 0.4 mL D_2O solution (20 mM NaCl, 5 mM PO_4, pH 5.8) were recorded at 10 °C. 2-D DQF-COSY, clean-TOCSY[27] (107 ms mixing time) and NOESY (350 ms mixing time) were recorded. The residual HOD signal was saturated by low power continuous irradiation. 2-D data sets were acquired with 2.05 s relaxation delay, 2.83 Hz resolution in F2 and 44 ms t_{1max} in F1 dimension, respectively. A 90° phase shifted sine bell was used in the t_2 and t_1 dimensions of NOESY, while a 30° phase shifted skewed sine bell was used prior to Fourier transformation of TOCSY and DQF-COSY spectra. The final spectral matrix consists of 2048 × 2048 data points.

(b) NMR spectra of the free duplex. The free duplex (~2 mM) was dissolved in an aqueous solution containing 5 mM sodium PO_4, 0.1 mM EDTA, pH 5.8. 2-D NOESY spectra of exchangeable protons were acquired at 5 °C (0.86 s relaxation delay, 150 ms mixing time, 12 kHz spectral window and 2048 × 512 data size). The acquisition times in t_2 and t_1 dimensions were 170 and 21 ms, respectively. The strong H_2O signal was suppressed using the Jump-Return pulse sequence[28] with a delay of 52 μs. 2-D NOESY spectra of non-exchangeable protons were acquired at 15 °C (3 s relaxation delay, 100 and 250 ms mixing times, 5 kHz

spectral window and 1024 × 512 data size). The acquisition times in t_2 and t_1 dimensions were 202 and 51 ms, respectively. DQF-COSY, COSY-35 and TOCSY (100 ms mixing time) data were obtained with a 2.6 s relaxation time while other parameters were identical to those used for the NOESY experiments, except that the t_2 acquisition time for the COSY-35 experiment was 405 ms for achieving higher digital resolution. Proton detected ^1H–^{31}P COSY spectrum[18] was obtained at 20 °C with a 1.5 s relaxation delay. The sweep width was 2000 Hz (3.33 ppm centered at HOD resonance) in the ^1H dimension (F2) and 1200 Hz (4.55 ppm centered at –3.15 ppm) in the ^{31}P dimension (F1). t_2 acquisition time and t_{1max} were 512 and 133 ms, respectively. All ^1H–^1H correlation data were processed as described in (a), while a 37.5° phase shifted qsine-bell was used in both the t_2 and t_1 dimensions to process the ^1H–^{31}P COSY data. No zero fill of data points was used throughout the process.

(c) The NCSi-glu–DNA complex. 2-D exchange spectra were recorded in D_2O (250 ms mixing time) and H_2O (200 ms mixing time) for sample I. 2-D ^1H–^{31}P COSY, ^1H DQF-COSY, TOCSY (100 and 150 ms) and NOESY (70, 100, 150 and 250 ms) spectra were recorded in D_2O and H_2O in the 5–20 °C temperature range for sample II. Data acquisition and processing were performed using similar conditions as described for the free duplex (*vide supra*) except that the relaxation delay for D_2O data was 2 s. NOE cross-peak volumes were measured using the FELIX program. Initially, the assignments were made through spin system and sequential connectivities which were well-defined. These assignments and a list of cross-peaks were cross-matched to give a table containing all possible assignments for each cross-peak in the 150 ms NOESY (collected on the AMX 750 MHz instrument). Manual screening of the cross-peak assignment table completed the NOE cross peak assignments. NMR results were finally used as restraints for structure elucidation of the complex as described in a separate report.[13]

Acknowledgements

This research is supported in part by the American Cancer Society (JFRA-493 to X. G.) and the NIH (CA44257 to I. H. G.). The 600 MHz NMR spectrometer at the University of Houston was funded in part by the W. M. Keck Foundation. The authors are grateful for the 750 MHz NMR instrument time provided by Bruker Analytische Messtechnik GMBH (Germany). J. G. thanks Professor M. Hogan (Baylor College of Medicine) for the postdoctoral support. Dr Collin Cross (UH) is acknowledged for the careful reading of the manuscript.

References and Notes

1. (a) Ishida, N.; Miyazaki, K.; Kumagai, K.; Rikimaru, M. *J. Antibiotics Ser.* **1965**, *A18*, 68; (b) Napier, M. A.; Holmquist, B.; Strydom, D. J.; Goldberg, I. H. *Biochem. Biophys. Res. Commun.* **1979**, *89*, 635; (c) reviewed in Dedon, P. C.; Goldberg, I. H. In: *Nucleic Acid Targeted Drug Design*, p. 475, Probst, C.; Perun, T. Eds; Marcel Decker; New York, 1992.

2. (a) Lam, K. S.; Hesler, G. A.; Gustavson, D. R.; Crosswell, A. R.; Veitch, J. M.; Forenza, S. *J. Antibiotics* **1991**, *44*, 472; (b) Otani, T.; Minami, Y.; Marunaka, T.; Zhang, R.; Xie, M.-Y. *J. Antibiotics* **1988**, *41*, 1580; (c) Schroeder, D. R.; Colson, K. L.; Klohr, S. E.; Zein, N.; Langley, D. R.; Lee, M. S. *J. Am. Chem. Soc.* **1994**, *116*, 9351; (d) Golik, J.; Clardy, J.; Dubay, G.; Groenewold, G.; Kawaguchi, H.; Konishi, M.; Krishnan, B.; Okhuma, H.; Saitoh, K.; Doyle, T. W. *J. Am. Chem. Soc.* **1987**, *109*, 3461; (e) Lee, M. D.; Dunne, T. S.; Siegel, M. M.; Chang, C. C.; Morton, G. O.; Borders, D. B. *J. Am. Chem. Soc.* **1987**, *109*, 3464; (f) Konishi, M.; Okhuma, H.; Tsuno, T.; Oki, T.; VanDune, G. D.; Clardy, J. *J. Am. Chem. Soc.* **1990**, *112*, 3715; (g) Zein, N.; Poncin, M.; Nilakantan, R.; Ellestad, G. A. *Science* **1989**, *244*, 697; (h) Nicolaou, K. C.; Dai, W.-M. *Angew. Chem. Int. Ed. Eng.* **1991**, *30*, 1387.

3. (a) Edo, K.; Mizugaki, M.; Koide, Y.; Seto, H.; Furihata, K.; Otake, N.; Ishida, N. *Tetrahedron Lett.* **1985**, *26*, 331; (b) Hensens, O. D.; Dewey, R. S.; Liesch, J. M.; Napier, M. A.; Reamer, R. A.; Smith, J. L.; Albers-Schonberg, G.; Goldberg, I. H. *Biochem. Biophys. Res. Commun.* **1983**, *113*, 538.

4. (a) Myers, A. G. *Tetrahedron Lett.* **1987**, *28*, 4493; (b) Myers, A. G.; Proteau, P. J. *J. Am. Chem. Soc.* **1989**, *111*, 1146.

5. Reviewed in Goldberg, I. H. *Acc. Chem. Res.* **1991**, *24*, 191.

6. (a) Kappen, L. S.; Goldberg, I. H. *Science* **1993**, *261*, 1319; (b) Kappen, L. S.; Goldberg, I. H. *Biochemistry* **1993**, *32*, 13138; (c) Hensens, O. D.; Chin, D.-H.; Stassinopoulos, A.; Zink, D. L.; Kappen, L. S.; Goldberg, I. H. *Proc. Natl Acad. Sci. U.S.A.* **1994**, *91*, 4534.

7. (a) Lee, M. D.; Ellestad, G. A.; Borders, D. B. *Acc. Chem. Res.* **1991**, *24*, 235; (b) Aiyar, J.; Hitchcock, S. A.; Denhart, D.; Liu, K. K.; Danishefsky, S. J.; Crothers, D. M. *Angew. Chem. Int. Ed. Engl.* **1994**, *33*, 854; (c) Li, T.; Zeng, Z.; Estevez, V. A.; Baldenius, K. U.; Nicolaou, K. C.; Joyce, G. F. *J. Am. Chem. Soc.* **1994**, *116*, 3709; (d) Xu, Y.; Zhen, Y.; Goldberg, I. H. *Biochemistry* **1994**, *33*, 5947.

8. (a) Galat, A.; Goldberg, I. H. *Nucleic Acids Res.* **1990**, *18*, 2093; (b) Sugiyama, H.; Fujiwara, T.; Kawabata, H.; Yoda, N.; Hirayama, N.; Sato, I. *J. Am. Chem. Soc.* **1992**, *114*, 5573; (c) Elbaum, E.; Schreiber, S. *Bioorg. Med. Chem.* **1994**, *4*, 309.

9. (a) Walker, S.; Murnick, J.; Kahne, D. *J. Am. Chem. Soc.* **1993**, *115*, 7954; (b) Paloma, L. G.; Smith, J. A.; Chazin, W. J.; Nicolaou, K. C. *J. Am. Chem. Soc.* **1994**, *116*, 3697.

10. (a) Langley, D. R.; Golik, J.; Krishnan, B.; Doyle, T. W.; Beveridge, D. L. *J. Am. Chem. Soc.* **1994**, *116*, 15; (b) Ikemoto, N.; Kumar, R. A.; Dedon, P. C.; Danishefsky, S. J.; Patel, D. J. *J. Am. Chem. Soc.* **1994**, *116*, 9387.

11. Dasgupta, D.; Goldberg I. H. *Biochemistry* **1985**, *24*, 6913.

12. (a) Povirk, L. F.; Goldberg, I. H. *Biochemistry* **1980**, *20*, 4773; (b) Povirk, L. F.; Dattagupta, N.; Warf, B. C.; Goldberg, I. H. *Biochemistry* **1981**, *20*, 4007.

13. Gao, X.; Stassinopoulos, A.; Rice, J. S.; Goldberg, I. H. *Biochemistry* **1995**, *34*, 40.

14. Stassinopoulos, A.; Goldberg, I. H. *Bioorg. Med. Chem.* **1995**, *3*, 713.

15. Freeman, R. *A Hand Book of Nuclear Magnetic Resonance*, Longman Scientific & Technical; New York; 1987; TCOSY p. 99; NOESY p. 111; COSY and DQF-COSY p. 233.

16. (a) Chin, D.-H.; Goldberg, I. H. *J. Am. Chem. Soc.* **1992**, *114*, 1914. Sample containing deuterium labeled at the Cys(Ha and Hb) positions was also used; (b) Chin, D.-H.; Goldberg, I. H. *Biochemistry* **1993**, *32*, 3611.

17. Much fewer NOEs were observed from the methyl thioglycolate activated NCS chromo (DMSO:D_2O in 2:1 ratio, 23°C); Myers, A. G.; Protean, P. J.; Handel, T. M. *J. Am. Chem. Soc.* **1988**, 110, 7212.

18. Sklenar, V.; Miyashiro, H.; Zon, G.; Miles, H. T.; Bax. A. *FEBS Letters* **1986**, *208*, 94.

19. Wuthrich, K. *NMR of Proteins and Nucleic Acids*, John Wiley; New York. 1986.

20. Majumdar A.; Hosur, R. V. *Prog. NMR Spectrosc.* **1992**, *24*, 109.

21. Gorenstein, D. G. *Phosphorus-31 NMR. Principles and Applications*, Academic Press; New York, 1984.

22. k_{ex} (s^{-1}) = exchanged species % / mixing time (s); exchanged species % = intensity of off-diagonal peak/intensity of diagonal peak.

23. (a) Gao, X.; Patel, D. J. *Q. Rev. Biophys.* **1989**, *22*, 93; (b) Gao, X.; Mirau, P.; Patel, D. J. *J. Mol. Biol.* **1992**, *222*, 819; (c) Krugh, T. R. *Curr. Opinion Str. Biol.* **1994**, *4*, 351. Drug–DNA interactions (d) Geierstanger, B. H.; Mrksich, M.; Dervan, P. B.; Wemmer, D. E. *Science* **1994**, *266*, 646.

24. (a) Meschwitz, S. M.; Goldberg, I. H. *Proc. Natl Acad. Sci. U.S.A.* **1991**, *88*, 3047; (b) Meschwitz, S. M.; Schultz, R. G.; Ashley, G. W.; Goldberg, I. H. *Biochemistry* **1992**, *31*, 9117.

25. Gao, X.; Jones, R. A. *J. Am. Chem. Soc.* **1987**, *109*, 1275.

26. Marion, D.; Wuthrich, K. *Biochem. Biophys. Res. Commun.* **1983**, *113*, 967.

27. States, D.; Haberkorn, R. A.; Ruben, D. J. *J. Magn. Reson.* **1982**, *48*, 286.

28. Greisinger, C.; Otting, G.; Wuthrich, K.; Ernst, R. R. *J. Am. Chem. Soc.* **1988**, *110*, 7870.

29. Nicholls, A.; Sharp, Kim.; Honig, B. *Proteins, Struct. Funct. Genetics* **1991**, *11*, 281.

(*Received in U.S.A.* 6 *December* 1994; *accepted* 20 *January* 1995)